Translational Oncology
www.transonc.com

Volume 3 Number 2 April 2010 pp. 114–122 **114**

Pheophorbide a–Mediated Photodynamic Therapy Triggers HLA Class I–Restricted Antigen Presentation in Human Hepatocellular Carcinoma[1]

Patrick Ming-Kuen Tang*,†, Ngoc-Ha Bui-Xuan*, Chun-Kwok Wong‡,§, Wing-Ping Fong¶,# and Kwok-Pui Fung*,§

*School of Biomedical Sciences, The Chinese University of Hong Kong, Shatin, N.T., Hong Kong, China; †Molecular Oncology, The Weatherall Institute of Molecular Medicine, University of Oxford, Oxford, United Kingdom; ‡Department of Chemical Pathology, The Chinese University of Hong Kong, Prince of Wales Hospital, Shatin, N.T., Hong Kong, China; §Institute of Chinese Medicine, The Chinese University of Hong Kong, Shatin, N.T., Hong Kong, China; ¶Department of Biochemistry, The Chinese University of Hong Kong, Shatin, N.T., Hong Kong, China; #Center of Novel Functional Molecules, The Chinese University of Hong Kong, Shatin, N.T., Hong Kong, China

Abstract

The immunomodulatory effects of photodynamic therapy (PDT) have been reported in several photosensitizers. Pheophorbide a (Pa), a chlorophyll derivative, shows antitumor effects on a number of human cancers in a PDT approach (Pa-PDT); however, the potential effect of Pa-PDT on the anticancer immunity has never been studied. In the present work, the underlying action mechanism of Pa-PDT was systemically investigated with a human hepatoma cell line HepG2. We found that Pa-PDT significantly inhibited the growth of HepG2 cells with a half maximal inhibitory concentration/endoplasmic reticulum of 0.35 μM at 24 hours by the induction of apoptosis, as shown by externalization of phosphatidylserine, release of mitochondrial cytochrome *c*, and activation of the caspases cascade in the treated cells. Interestingly, using two-dimensional polyacrylamide gel electrophoresis analysis, a 57-kDa disulfide-isomerase–like ER resident protein (ERp57) that belongs to the HLA class I–restricted antigen-processing machinery was found to be mediated during the Pa-PDT treatment. This activation of antigen presentation was confirmed by Western blot analysis and immunostaining. Furthermore, a cross-presentation of antigen with HLA class I proteins and 70-kDa heat shock protein was found in Pa-PDT–treated cells, as shown by the confocal microscopic observation and immunoprecipitation assay. Nevertheless, the immunogenicity of HepG2 cells was increased by Pa-PDT treatment that triggered phagocytic capture by human macrophages. Our findings provide the first evidence that Pa-PDT can trigger both apoptosis and cancer immunity in the tumor host.

Translational Oncology (2010) 3, 114–122

Introduction

Photodynamic therapy (PDT) is a recently developed modality for tumor treatment. It is currently used in the treatment of many cancers including lung cancer, head and neck cancers, liver metastases, cholangiocarcinoma, and prostrate cancer [1]. This approach has also been applied to treat various diseases, including psoriasis, rickets, vitiligo, and skin cancer by ancient Egyptian, Indian, and Chinese thousands of year ago [2,3]. PDT requires the simultaneous presence of photosensitizer and light, both are nontoxic individually, to induce rapid cytotoxicity on the target tissue in the presence of oxygen where the inhibitory effects of PDT can be achieved by inducing

Address all correspondence to: Dr. Kwok-Pui Fung, School of Biomedical Sciences, The Chinese University of Hong Kong, Shatin, N.T. Hong Kong, China. E-mail: kpfung@cuhk.edu.hk

[1]This project was supported by the earmarked grants from Research Grants Council, Hong Kong, China (Project code: 464507); South China National Research Centre for Integrated Biosciences in Collaboration with Zhongshan University (Project code: 1902006); Ming Lai Foundation; The International Association of Lion Clubs District 303 – Hong Kong, and Macau Tam Wah Ching Chinese Medicine Resource Center in Institute of Chinese Medicine, CUHK; and Focused Investment on Biomedical Sciences Scheme of CUHK.

Received 2 September 2009; Revised 20 October 2009; Accepted 28 October 2009

DOI 10.1593/tlo.09262

apoptosis [4,5]. Enhancement of systemic antitumor immunity is another important strategy in cancer treatment. Recently, numerous preclinical studies have found that local PDT treatment can enhance anticancer immunity through the activation of neutrophils and natural killer cells [6,7] because of the induction of acute inflammation, expression of heat shock proteins (HSPs), invasion, and infiltration of the tumor by leukocytes, which might increase the presentation of tumor-derived antigens to T cells [8].

Pheophorbide a (Pa), a derivative of chlorophyll *a*, is a breakdown product during the turnover of chlorophyll *a* in plant cells [9]. Our previous study has identified Pa as the active component in the antiproliferative effect of a traditional Chinese medicine *Scutellaria barbata* on human hepatoma Hep3B cells [10]. It has also been reported as a photocytotoxic component of *Thunbergia laurifolia* Lindl and *Aglaonema simplex* [11,12]. Pa generates singlet oxygen to trigger cancer cell death during irradiation in the presence of oxygen. The effect of Pa-based PDT (Pa-PDT) has been demonstrated on a number of human cancer cells, including Jurkat leukemia, pigmented melanoma, colonic cancer, and pancreatic carcinoma [13–16]. The efficacy of Pa-PDT on hepatocellular carcinoma has been evaluated *in vivo*, and its antitumor effect has also been demonstrated *in vitro* on the hepatitis B virus–induced human hepatoma cell line Hep3B as well as on the hepatitis C virus–induced human hepatoma cell line with multidrug resistance property in our previous studies, where the induction of mitochondrial-dependent apoptosis is suggested to be a common pathway for Pa-PDT on human hepatoma treatments [17–20].

The immunomodulatory effects of PDT, including both immunostimulation and immunosuppression, have been reported in several photosensitizers [3,6,7]. These phenomena may further enhance the therapeutic efficiency on both primary and metastasis cancers in antitumor PDT [21]. Pa is a well-studied second-generation photosensitizer; however, its potential effects on immunity have not yet been studied. Our present work was done with a proteomic approach to reveal the potential effect of Pa-PDT on cancer immunity by using the human hepatoma cell line HepG2 as an *in vitro* model. The results demonstrated that Pa-PDT triggered the antigen presentation together with apoptosis in the treated HepG2 cells. This study provides the first reference of the immunomodulatory effect of Pa-PDT on human cancer cells *in vitro*.

Materials and Methods

Materials

Culture media were purchased from Invitrogen (Carlsbad, CA). All other chemicals were purchased from Sigma Chemical Co (St. Louis, MO). Pa originally purified from *S. barbata* [10] is now commercially available. Pa used in this study was purchased from Frontier Scientific (Logan, UT).

Cell Cultures

Human hepatocellular carcinoma HepG2 cells (American Type Culture Collection, ATCC, Manassas, VA) were cultured in RPMI 1640, and human normal hepatic cells WRL-68 (ATCC) were maintained in minimum essential medium. All media contained 10% (vol./vol.) fetal bovine serum, 100 U/ml penicillin G, and 100 μg/ml streptomycin. Sodium pyruvate (1 mM) was exclusively added into the minimum essential medium. The cells were incubated at 37°C in a humidified atmosphere of air/CO_2 (95%:5%).

Irradiation of Photosensitizer

Cells were preloaded with Pa for 2 hours. After washings, the cells were photoirradiated for 20 minutes using a 600-W quartz-halogen lamp that is attenuated by a 10-cm layer of water and a long-pass 610-nm filter. The light intensity was 70 mW/cm^2 (i.e., 20 minutes of irradiation = 84 J/cm^2) [17–19].

Effects of Pa-PDT on Cell Viability

Cells (1×10^4 per well) were seeded in a 96-well culture plate and incubated for 24 hours to allow attachment. After washing with PBS, the cells were incubated with the appropriate concentrations of Pa followed by photoactivation. After 48 hours, the cells were washed gently with phosphate-buffered saline (PBS). Thirty microliters of methyl-thiazoldiphenyl tetrazolium (MTT) (5 mg/ml) was added to each well and incubated for 2 hours at 37°C. Then, the MTT solution was replaced by 100 μl of dimethyl sulfoxide in each well. Absorbance was measured with a microtiter plate reader (Bio-Rad, Hercules, CA) at 540 nm, and all data were calculated as percentage of control.

Measurement of Phosphatidylserine Translocation

HepG2 cells (3×10^5 per well) were seeded in a six-well culture plate and collected 1 hour after the PDT treatment as described in our previous study [22]. The cells were stained with the annexin V–fluorescein isothiocyanate (FITC) kit (Trevigen, Gaithersburg, MD) and analyzed by FACSort flow cytometry (Becton Dickinson Bioscience Corp, San Jose, CA) with the CellQuest software (BD Biosciences). The cell population was gated by forward scatter and side scatter, and the fluorescence signals were acquired by the FL1 and FL3 channels in log scale.

Western Blot Analysis

The method described previously was used [22,23]. The PDT-treated cells (3×10^6 per dish) collected at 4 hours after PDT were extracted with the whole-cell extraction buffer (2% sodium dodecyl sulfate [SDS], 10% glycerol, 625 mM Tris-HCl [pH 6.8], β-mercaptoethanol [5% vol./vol.]) and subjected to gel electrophoresis. The expressions of target proteins were monitored with primary antibodies against β-actin (1:5000), HLA class I (1:1000; Sigma), p53 (1:1000), procaspase-3 (1:1000), procaspase-8 (1:1000; Santa Cruz Biotechnology, Santa Cruz, CA), procaspase-9 and caspase-9 (1:1000; Stressgen, Ann Arbor, MI), ERp57 (1:1000), HSP70 (1:5000; Abcam, Cambridge, UK), and calreticulin (CRT) (1:5000; Abcam). For the measurement of cytochrome *c* release, the cytosolic protein was collected with the lysis buffer (75 mM NaCl, 1 mM NaH_2PO_4, 8 mM Na_2HPO_4, 250 mM sucrose, 21 μg/ml aprotinin, 5 μg/ml leupeptin, 1 mM phenylmethylsulfonyl fluoride, and 25 μg digitonin), and the supernatant collected was used for Western blot analysis with primary antihuman cytochrome *c* antibody (1:1000; Santa Cruz). The protein content of each sample was normalized by the corresponding β-actin level. After incubating with the secondary antibody conjugated with horseradish peroxidase, the immunodetected proteins were visualized by using an enhanced chemiluminescence assay kit (Amersham Life Science, Pittsburgh, PA).

Two-dimensional Gel Electrophoretic Analysis

Cells (1×10^6) were seeded in a 100-mm culture dish and incubated for 24 hours to allow attachment. Four hours after 0.4 μM Pa without PDT (control) or 0.4 μM Pa-PDT treatment, the cells were collected and washed five times with cell washing buffer (10 mM Tris-base, 250 mM sucrose, pH 7.4). The cells were lysed in the lysis buffer (8 M urea, 4% CHAPS, 2% pharmalyte 3-10), and 150 μg of

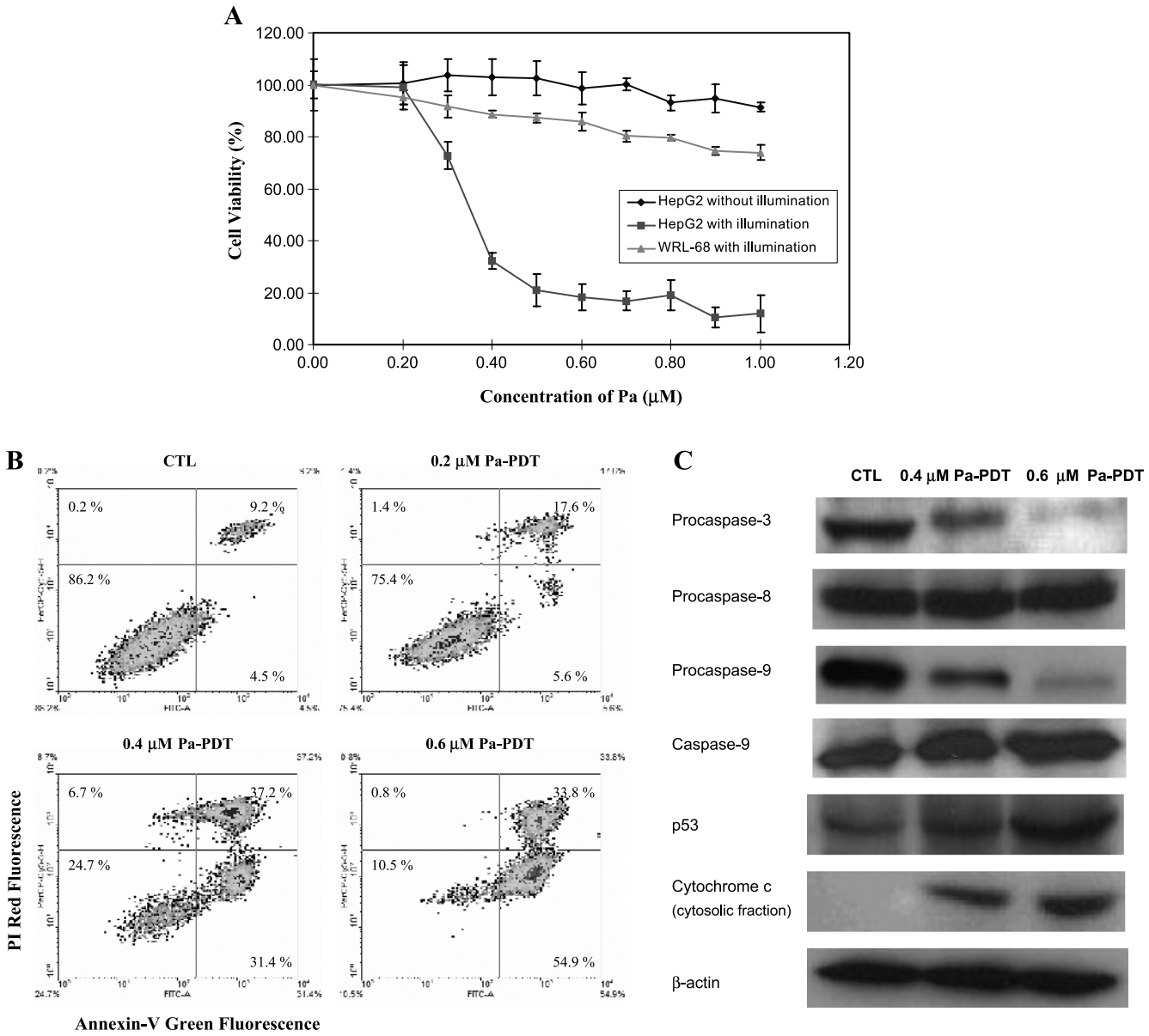

Figure 1. Activation of mitochondrial-mediated apoptosis in Pa-PDT treated HepG2 cells. (A) *In vitro* inhibitory effect of Pa-PDT in HepG2 and WRL-68 cells. The cells (1×10^4 per well) were preincubated with Pa in a 96-well plate for 2 hours and then received light illumination (84 J/cm^2) for 20 minutes. In the control group, Pa-treated HepG2 cells received no light illumination. Cell survival was assessed by MTT assay 24 hours after treatment. Results are mean ± SD of three independent experiments. (B) Externalization of PS in Pa-PDT–treated cells. The cells were collected at 1 hour after treatment and stained with the annexin V–FITC and PI costaining kit. The cells were submitted to flow cytometry, where the percentages of cell population in each quadrant were shown as mean in the figures of five independent experiments. (C) Change in the expression level of apoptotic proteins in Pa-PDT–treated HepG2 cells. Cells (3×10^6) were treated with solvent (0.04% ethanol [CTL]) or Pa (0.4 and 0.6 μM) for 2 hours and then with light illumination (84 J/cm^2) for 20 minutes. Twenty-four hours after treatment, the whole-cell lysates were prepared, and the change in the level of various apoptosis-related proteins was analyzed using Western blot analysis. For the release of mitochondrial cytochrome *c*, the cytosolic protein was collected 1 hour after treatment. The housekeeping protein β-actin was also probed for normalization. Data shown are representative of five independent experiments.

protein of the collected supernatant was subjected to first-dimension isoelectric focusing with a 13-cm immobilized pH gradient (pH) strip (pH 3-10 Immobiline DryStrip; Amersham Biosciences, Pittsburgh, PA) by using the Ettan IPGphor Isoelectric Focusing Unit (Amersham Biosciences) with the following profile: 30 V for 10 hours (gradient), 200 V for 1 hour (step-and-hold), 500 V for 1 hour (step-and-hold), 8000 V for 30 minutes (gradient), 8000 V for 6.5 hours (step-and-hold) until a total of 60,000 V-h had been achieved. The IPG strips were then subjected to the second-dimension electrophoretic analysis with a 10% SDS polyacrylamide gel electrophoresis (two-dimensional SDS-PAGE) by using the SE 600 Ruby Electrophoresis Unit (Amersham Biosciences) at a constant 150 V, and the collected gel was finally stained by using PlusOne Silver Staining Kit (Amersham Biosciences). The results were analyzed by the software Image Master 2D version 2.0 (Amersham Biosciences). The mediated protein spots were excised from the gel and finally identified by Matrix assisted laser

desorption-ionization time-of-flight mass spectrometry (MALDI-TOF MS) [24].

Immunohistochemistry

Cells (3×10^5 per well) were grown on the coverslips. The PDT-treated cells were fixed with chilled fixation buffer (70% methanol and 30% ethanol) at −20°C for 20 minutes and then blocked with TBS with 0.1% of Tween 20 that contains 10% fetal bovine serum at 4°C for 30 minutes as described in our previous study [18]. The fixed samples were incubated overnight at 4°C with monoclonal anti–HLA class I antibody (1:500; Sigma), or rabbit anti–HLA class I and mouse anti-HSP70 antibodies (Abcam) and then incubated with FITC-conjugated goat antimouse immunoglobulin G or both with *R*-phycoerythrin–conjugated antirabbit (1:500; Zymed, South San Francisco, CA) antibodies for a further 2 hours. Finally, the samples were washed three times with TBS with 0.1% of Tween 20 and observed under a Nikon TE2000 fluorescence microscope (Nikon, Badhoevedrop, The Netherlands) with an excitation wavelength at 490 nm and an emission wavelength at 516 nm or were viewed under a Leica SP5 confocal microscope (Leica, Wetzlar, Germany) where Alexa Fluor 594 and FITC fluorescence was detected by using appropriate excitation (490 and 578 nm) and emission (516 and 610 nm) wavelengths. HLA class I proteins were assigned as red, and HSP70 proteins were shown in green. Images were merged together by using the MetaMorph software (Universal Imaging Corp, Downingtown, PA).

Immunoprecipitation

The PDT-treated cells (3×10^6 per dish) collected at 4 hours after PDT were lysed by incubating in 1 ml of nondenaturing lysis buffer (20 mM Tris-HCl, pH 8, 137 mM NaCl, 10% glycerol, 1% Triton X-100, 2 mM EDTA, and 20 μg/ml aprotinin) for 30 minutes at 4°C. The supernatant was collected after centrifuging for 20 minutes at 12,000*g*. The collected cell lysate (200 μg) was incubated with anti–HLA class I antibody (Abcam) at 4°C overnight, and then 70 μl of preswollen protein-A–conjugated beads was added into the sample and incubated for 4 hours. After removing the supernatant and washing with lysis buffer three times, 25 μl of whole-cell extraction buffer was added to denature the protein and separate it from the protein-A beads. The samples were eventually analyzed by Western blot assay with anti-HSP70 antibody to study the interaction between HSP70 and HLA class I proteins.

Phagocytic Activity Assays of Human Macrophage

Fresh human buffy coat obtained from healthy volunteers of Hong Kong Red Cross Blood Transfusion Service was diluted two-fold with PBS at 4°C and centrifuged using an isotonic Percoll solution (density 1.082 g/ml; Amersham and Pharmacia Biotech, Uppsala, Sweden) for 30 minutes at 1000*g* without deceleration. After centrifugation, four layers of fluids appeared in the column. The thin white interface between the top and third layers containing the viable peripheral blood mononuclear cells including lymphocytes and monocytes was collected. The collected peripheral blood mononuclear cells were cultured with RPMI for 2 hours, and the adherent cells in the culture flask were used as human macrophages [25]. The phagocytosis of human macrophages was evaluated using a commercial kit (Vybrant Phagocytosis Assay Kit; Invitrogen). The intensities of fluorescence were acquired by a FLUOstar Galaxy plate reader (BMG Labtech, Offenburg, Germany).

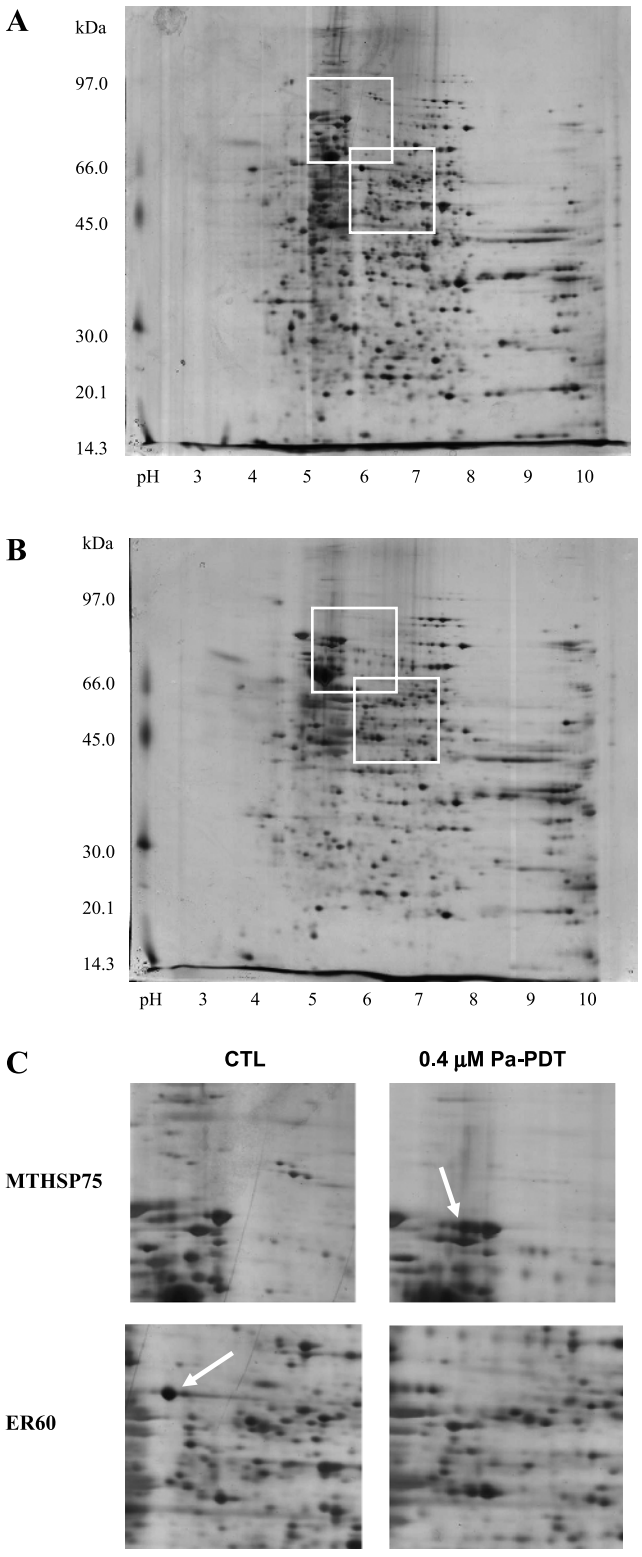

Figure 2. Protein expression profile of Pa-PDT–treated HepG2 cells. The total proteins of (A) 0.4 μM Pa (dark control) and (B) 0.4 μM Pa-PDT–treated HepG2 cells were extracted at 4 hours after illumination. The protein samples were subjected to isoelectric focusing, then separated on a 10% SDS-PAGE gel, and finally visualized by silver staining. The gel result was analyzed by the software Image Master. (C) Enlarged regions showing the positions and identities of the differentially expressed proteins MTHSP75 and ER60 in HepG2 cells after Pa-PDT treatment. The figure is a representative of five trials.

Table 1. The Differentially Expressed Proteins Mediated by Pa-PDT Treatment in HepG2 Cells.

Protein Name	M_W (kDa)	PI	Protein Score	CI (%)
Upregulated				
Chaperonin	61.016	5.70	205	100.00
Heat shock 70-kDa protein 9B, precursor (MTHSP75)	73.734	5.97	179	100.00
Chain A, heat shock 70-kDa protein 42-kDa ATPase N-terminal domain (HSP70)	41.802	6.69	170	100.00
Prohibitin	29.786	5.57	161	100.00
HnRNP protein A2	35.984	8.67	92	100.00
Unnamed protein product (gi 10436678)	30.143	9.23	91	99.99
LEKTI precursor	120.693	8.39	90	99.99
CTCL tumor antigen se2-1	93.443	5.37	83	99.96
KIAA1640 protein	108.677	6.33	79	99.89
Myosin heavy chain, skeletal muscle, fetal (myosin heavy chain Iib)	222.874	5.67	72	99.39
Zinc finger protein 2	72.326	8.99	72	99.48
30S ribosomal protein S7 homolog	28.144	10.00	72	99.46
Disulfide isomerase ER 60 (ERp57)	56.748	5.88	71	99.30
Serine protease inhibitor Kazal-type 5 precursor	120.681	8.50	68	98.73
Bone marrow zinc finger protein 2	72.113	9.02	67	98.36
Zinc finger protein 311	69.930	9.16	66	98.03
DNA-binding protein	179.967	9.32	66	97.89
Tumor necrosis factor type 2 receptor–associated protein	55.758	8.19	60	90.55
Downregulated				
Heat shock 70-kDa protein 8 isoform 2	53.484	5.62	186	100.00
Enolase 1 (alpha) protein (ENO1)	47.139	7.01	165	100.00
Phospholipase C-alpha	56.666	6.23	149	100.00
Protein disulfide isomerase–associated 3 precursor (ER-60)	56.740	5.88	142	100.00
Desmoplakin (DP)	331.570	6.44	103	100.00
Pyruvate kinase (EC 2.7.1.40)	57.966	7.20	103	100.00
Adenylate kinase 3	25.252	8.47	97	100.00
Triosephosphate isomerase (TIM)	26.609	7.10	96	100.00
Myosin heavy chain (MyHC-Iib)	222.000	5.67	92	100.00
Stress-induced phosphoprotein 1 (HSP70/HSP90-organizing protein)	62.599	6.40	92	100.00
Plectin	64.921	5.38	88	99.00
Tropomyosin isoform	28.938	4.79	83	99.96
Mitosin	357.063	5.06	72	99.47
Desmoplakin (DP)	33.200	6.44	68	98.67
KIAA1081 protein	115.038	5.96	66	97.93
WW domain binding protein 5	12.741	5.35	62	94.31
Cytosolic thyroid hormone-binding protein	57.964	7.95	62	94.44

The Pa-PDT–regulated proteins identified from two-dimensional gel electrophoresis and MALDI-TOF MS analysis were listed according to their protein scores (significant when >59) and confidence interval (CI).

Statistical Analysis

Data were presented as mean ± SD of various numbers of experiments. Statistical analysis was performed by one-way analysis of variance with Bonferroni *post hoc* test (two-tailed). $P < .05$ was considered statistically significant.

Results

Cytotoxicity of Pa-PDT on Human Hepatoma HepG2 Cells and Normal Human Hepatic WRL-68 Cells

The antitumor effect of Pa-PDT was examined on the human hepatocellular carcinoma cell line HepG2. A dose-dependent growth inhibitory effect was shown on HepG2 cells with a half maximal inhibitory concentration (IC_{50}) of 0.35 μM at 24 hours (Figure 1*A*). The normal human hepatic cells WRL-68 were much more resistant to the Pa-PDT effect: the cell viability was approximately 74% at a drug concentration of 1.0 μM (Figure 1*A*), and this result is consistent to that of our previous study [18].

Activation of Intrinsic Apoptotic Pathway in Pa-PDT–Treated HepG2 Cells

Translocation of membrane protein phosphatidylserine (PS) is a hallmark of apoptotic cells, and this phenomenon was observed on the Pa-PDT–treated HepG2 cells in a dose-dependent manner. As shown in Figure 1*B*, 31.4% and 54.9% of early apoptotic cells (annexin V–FITC–positive and propidium iodide–negative) were found in HepG2 cells after treating with 0.4 and 0.6 μM Pa-PDT, respectively, but only 4.5% in the control sample. For late apoptotic cells (annexin V–FITC–positive and propidium iodide–positive), the percentage of cell population was more than 30% in samples treated with 0.4 or 0.6 μM Pa-PDT, whereas only 9.2% appeared as late apoptotic cells in the control (Figure 1*B*). In addition, as shown in Figure 1*C*, cytochrome *c* in the cytosolic fraction was significantly increased, implying a release of mitochondrial cytochrome *c* in the Pa-PDT–treated cells. Nevertheless, the levels of procaspase-3 and -9 were decreased with inductions of p53 and caspase-9 expression, whereas the level of procaspase-8, responsible for the extrinsic apoptotic pathway, was relatively unchanged after 0.4 and 0.6 μM Pa-PDT (Figure 1*C*). Our findings confirmed that Pa-PDT induced apoptosis in HepG2 cells through the mitochondria-mediated pathway.

Identification of Pa-PDT–Mediated Protein Expression in HepG2 Cells

To find out pathways that are potentially mediated by Pa-PDT, protein lysate of Pa alone (dark control) and Pa-PDT–treated HepG2 cells were analyzed by two-dimensional PAGE, and the induced protein spots were detected by the PDQuest software (Bio-Rad). Fifty-one protein spots exhibited significantly different expression levels in the

0.4 μM Pa-PDT–treated sample (Figure 2*B*) when compared with the dark control (0.4 μM Pa with PDT; Figure 2*A*). Among them, 35 protein spots were successfully identified by MALDI-TOF MS analysis. Eighteen of them were upregulated, whereas 17 were downregulated after the Pa-PDT treatment (Table 1). The expression changes of an identified upregulated spot heat shock 70 kDa protein 9B precursor (MTHSP75) and an identified downregulated spot protein disulfide isomerase-associated 3 precursor (ER60) were illustrated in Figure 2*C*.

Induction of Antigen-Processing Machinery in Pa-PDT–Treated HepG2 Cells

The activation of the antigen presentation machinery, in which MTHSP75 and ER60 are involved [26], in Pa-PDT–treated HepG2 cells was further confirmed by Western blot analysis. As shown in Figure 3*A*, both HSP70, the active form of MTHSP75, and ERp57, the cleavage form of ER60 protein, were increased in a dose-dependent manner. The levels of HLA class I and CRT, proteins for the ERp57-mediated antigen processing machinery, were also increased in a dose-dependent manner after Pa-PDT treatment. The increase in the expression of HLA class I protein was also obvious under a fluorescent microscope, which showed a plasma membrane localization (Figure 3*B*). The immunogenicity of Pa-PDT–treated cells was evaluated by coincubation with human macrophages.

Involvement of HSP70 in HLA Class I–Mediated Antigen Presentation during Pa-PDT

The involvement of HSP70 on antigen presentation is still controversial. The potential interaction of HSP70 with HLA class I protein was investigated in the present study. Subcellular localization of HLA class I protein and HSP70 was revealed by immunostaining. Using confocal microscope, the fluorescence of HSP70 and HLA class I protein was concentrated on the plasma membrane (Figure 4*A*), and these images overlapped well with each other (Figure 4*B*). The interaction of HSP70 and HLA class I protein was further confirmed by an immunoprecipitation method. HSP70 was detected in immune complexes precipitated with antibody specific for HLA class I from

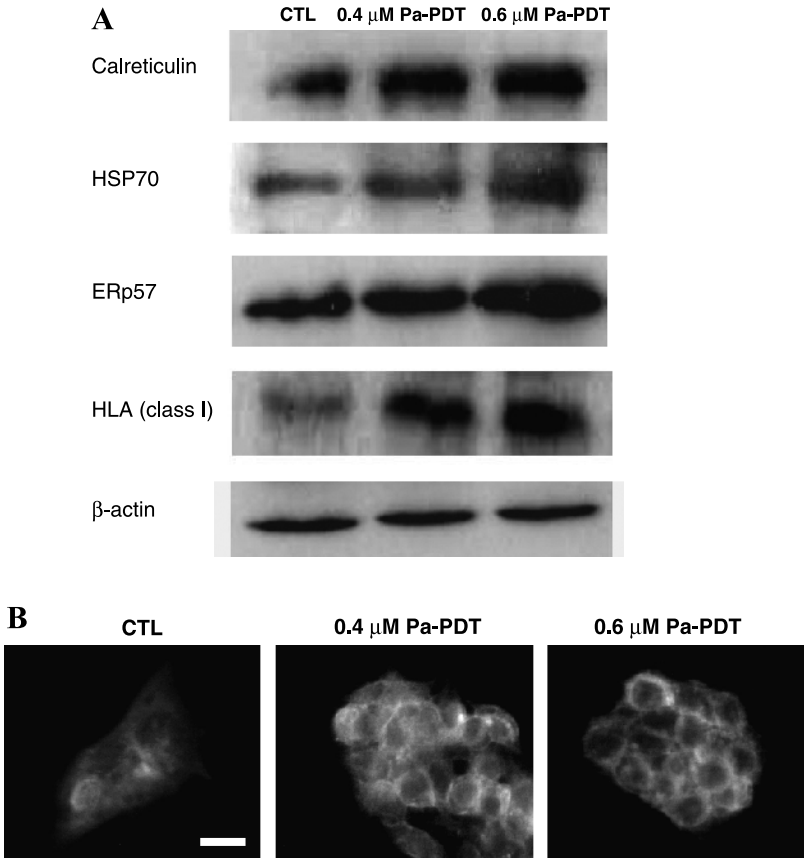

Figure 3. Induction of antigen presentation by Pa-PDT treatment. (A) Change in the expression level of proteins related to antigen presentation machinery in Pa-PDT–treated HepG2 cells. Cells (3×10^6) were treated with solvent (0.04% ethanol [CTL]) or Pa (0.4 and 0.6 μM) for 2 hours and then with light illumination (84 J/cm^2) for 20 minutes. Four hours after treatment, the whole-cell lysates were prepared, and the expression levels of various related proteins were analyzed using Western blot. The housekeeping protein β-actin was also probed for normalization. Data shown are representative of five independent experiments. (B) The induction of HLA class I protein expression in Pa-PDT–treated HepG2 cells. The Pa-PDT–treated cells (5×10^4 per well) were fixed at 24 hours after treatment and overnight immunostained with monoclonal anti–HLA class I antibody. The stained cells were probed with FITC-conjugated secondary antibody for 2 hours before observation under a Nikon TE2000 fluorescence microscope. Fluorescence micrographs were acquired with an excitation wavelength at 400 to 440 nm and an emission wavelength at 590 to 650 nm. The images are representatives of three independent trials. Bar, 20 μm.

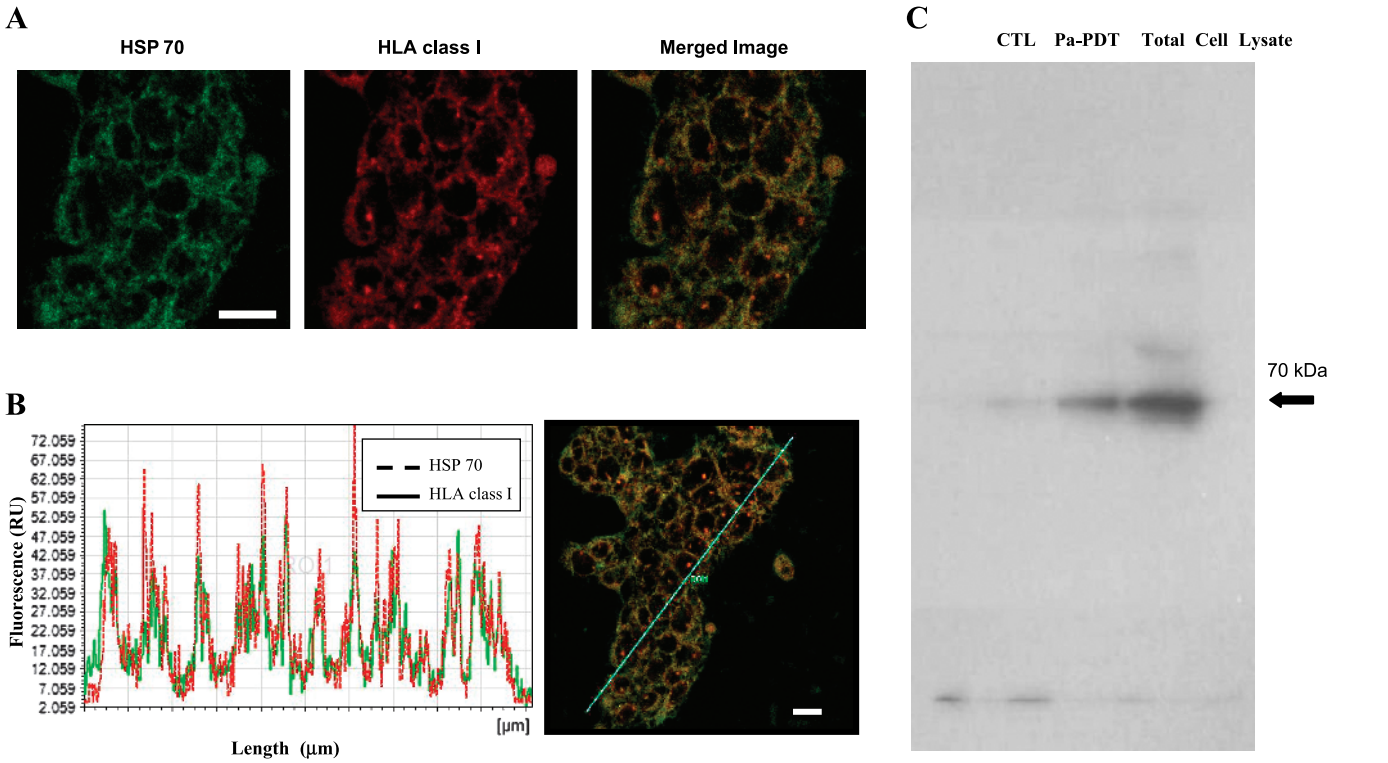

Figure 4. Association of HSP70 with HLA class I protein in Pa-PDT–treated HepG2 cells. (A) Intracellular tracking of fluorescence-labeled HSP70 and HLA class I proteins using confocal microscopy. HepG2 cells were treated with 0.6 μM Pa-PDT, fixed at 24 hours after illumination, and overnight immunostained with monoclonal anti-HSP70 and anti-HLA class I antibodies. The stained cells were then further probed with secondary antibody that is either FITC- or Alexa Fluor 594–conjugated for 2 hours before observation. Fluorescence micrographs were acquired with a Leica SP5 confocal microscope, where HSP70 was assigned as green (left panel with a scale bar = 20 μm), and the HLA class I protein was assigned as red (middle panel). In the merged image, colocalization of HSP70 and HLA class I protein showed yellow color (right panel). (B) Quantification of protein colocalization. Confocal merged images (right panel) and fluorescence topographic profiles (left panel) of Pa-PDT–treated HepG2 cells costained with anti-HSP and anti–HLA class I protein antibodies were shown. The green rod (ROM) indicates the analyzed longitudinal transcellular zone. (C) Coimmunoprecipitation of HLA class I interacting proteins in Pa-PDT–treated HepG2 cells. The samples CTL (solvent control) and 0.6 μM Pa-PDT–treated HepG2 cells (Pa-PDT) were collected at 4 hours after PDT treatment and immunoprecipitated with anti–HLA class I antibodies, and the total HepG2 cell lysate were collected without the immunoprecipitation step and used as a positive control for the anti–HSP70 antibody (Total Cell Lysate) followed by SDS-PAGE and immunoblot analysis with anti–HSP70 antibodies. Data are representative of three independent trials.

Pa-PDT–treated HepG2 cells lysate (Figure 4*C*). Our data suggested that HSP70 was recruited by HLA class I protein during Pa-PDT treatment in HepG2 cells.

Induction of Phagocytic Activity of Human Macrophages by Pa-PDT–Treated HepG2 Cells

In addition, the effect of Pa-PDT treatment on immunogenicity of human cancer cells was investigated in this study. As shown in Figure 5, the phagocytic activity of the macrophages was increased by approximately two-fold with the addition of Pa-PDT treated HepG2 cells. Interestingly, the phagocytic activity was significantly decreased to 27.1% in the sample where HepG2 cells were treated with solvent only ($P < .05$). Our study therefore demonstrated that Pa-PDT treatment would also give a positive influence on the phagocytic capture and ingestion of human hepatoma HepG2 cells by macrophages.

Discussion

Pa is a well-studied second-generation photosensitizer that establishes its antitumor effects on cancer cells through apoptosis induction [17–20]. The inhibitory effect of Pa-PDT was specifically shown on human hepatoma cells in this study. Pa-PDT acted on HepG2 cells with the IC_{50} value of 0.35 μM at 24 hours, whereas 73.9% and 91.4% cell survival rates were found in the human normal hepatic cells WRL-68 treated with 1.0 μM Pa-PDT and HepG2 cells with 1.0 μM Pa treatment alone (without light illumination), respectively (Figure 1*A*). Conversely, a commercial photosensitizer zinc (II) phthalocyanine had higher cytotoxicity in PDT on WRL-68 than HepG2 cells, the IC_{50} values being 0.7 and 1.3 μM, respectively, at 24 hours (data not shown). The difference in the cytotoxicity of Pa-PDT and zinc (II) phthalocyanine in human hepatoma and normal hepatic cells might be related to the subcellular localization of the photosensitizers. Zinc (II) phthalocyanine was found in Golgi apparatus [27], but Pa was concentrated in mitochondria [17,18]. In addition, Pa was reported to have an additional mode of protection by increasing the detoxification glutathione-*S*-transferase gene expression on normal liver cells, thus making Pa-PDT less cytotoxic on WRL-68 cells [28]. Furthermore, a similar phenomenon was suggested by Evrard et al. [29] that Pa-PDT showed selective cytotoxicity on the pancreatic rat carcinoma with an *in vivo* model study. Mechanistic study of Pa-PDT–mediated cell death on HepG2 cells was carried out in the present study. The hallmark

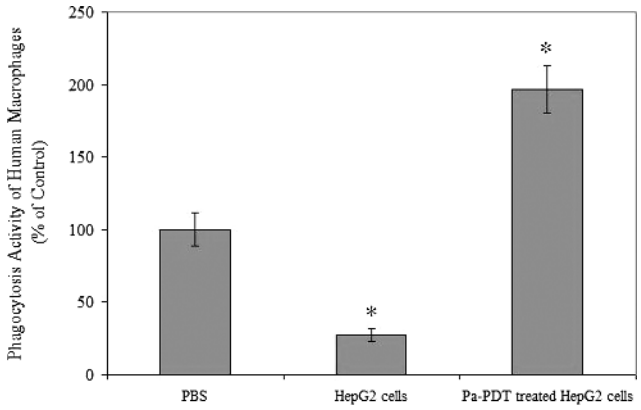

Figure 5. Induction of human macrophages phagocytic activity by Pa-PDT–treated cells. The HepG2 cells were Pa-PDT treated, collected at 2 hours, and then resuspended in PBS (2×10^6 cells/ml). The human marcophages (5×10^4 cells per well) in the 96-well culture plate were incubated with 100 μl of PBS (PBS), cell lysates of HepG2 treated with 0.04% ethanol as solvent control (HepG2 cells), or cell lysate of Pa-PDT–treated HepG2 cells (Pa-PDT–treated HepG2 cells) for 1 hour, and then the phagocytosis activities of human marcophages were measured by the Vybrant Phagocytosis Assay Kit. Data are shown as mean ± SD of three independent experiments (*$P < .05$, when compared with the PBS only control).

phenomenon of apoptosis, PS externalization, was found (Figure 1*B*), and the mitochondrial-mediated apoptotic pathway was shown to be activated (Figure 1*C*) in the Pa-PDT–treated sample. Our results suggested that Pa-PDT induced cancer cell death mainly by induction of apoptosis through the intrinsic apoptotic pathway in HepG2 cells as it does in other cancer cells [13–20]. Pa-PDT has a significant therapeutic potential and it could possess selectivity for human hepatoma cells.

The importance of immune system in PDT on cancer treatment has been raised recently. Spontaneous regression in advanced tumors including hepatocellular carcinoma has been reported and the significances of PDT on immunostimulation or immunosuppression have been well documented [30–33]. It inspires an ideal cancer therapy that can give direct cytotoxicity to the tumor cells and trigger the immune reorganization of cancer cells at the same time. So, the therapeutic potential of Pa-PDT on cancer immunity was investigated in this study. Protein expression profile of Pa-PDT–treated HepG2 cells was analyzed by using two-dimensional PAGE (Figure 2, *A* and *B*); the identified Pa-PDT–regulated proteins were classified according to several functional categories, including antigen presentation (e.g., ER60), HSP (e.g., chaperonin, MTHSP75), cell death pathway (e.g., tumor necrosis factor type 2 receptor–associated protein) as well as those with unknown function (Table 1). The identified proteins MTHSP75 and ER60 with high protein scores in the MALDI-TOF MS analysis were chosen for further study (Figure 2*C*).

Protein MTHSP75 is the precursor of HSP70. *In situ* HSP70 overexpression is known to enhance DC antigen presentation and overcome host immune tolerance to tumor antigens. It is involved in antigen presentation and antitumor immune responses by cooperating with the antigen presentation cells [34,35]. ER60 is the precursor of protein disulfide isomerase ERp57 that functions together with calnexin, CRT, and tapasin as a molecular chaperone in glycoprotein biosynthesis, including the generation of a stable HLA class I–peptide complex in the ER [36,37]. Our results demonstrated that the activation of ERp57-mediated pathway occurred during Pa-PDT treatment where the HLA class I–restricted antigen presentation machinery was triggered and the expression of HLA class I protein was upregulated on the plasma membrane of the treated HepG2 cells (Figure 3, *A* and *B*). Our findings suggest that Pa-PDT can trigger antigen presentation in the treated cancer cells to stimulate the host immune response.

Furthermore, the Pa-PDT–triggered antigen presentation was found to work together with HSP70 (Figure 4, *A* and *B*) in the treated HepG2 cells. The interaction of HSP70 and HLA class I protein was confirmed by the coimmunoprecipitation assay (Figure 4*C*). Recently, HSP70 is suggested to be involved in antigen presentation during PDT treatments. It forms stable complexes, cross-presents the tumor antigens with HLA proteins, resulting in an antigen-specific T-cell stimulation in the cancer host [35,38,39]. Nevertheless, there is a new approach for developing tumor vaccines by using PDT-treated cancer cell lysates, and Pa-PDT should be considered as one of the candidates [40]. Our results supported that HSP70 was upregulated and collaborated with the HLA class I proteins to enhance the antigen presentation efficiency in the Pa-PDT–treated cells.

Nevertheless, the effect of Pa-PDT–induced immunogenicity of human liver cancer cells was also demonstrated with primary human macrophages; as shown in Figure 5, a significant increase of phagocytic activity was found when the macrophages were coincubated with Pa-PDT–treated HepG2 cells. Interestingly, an inhibitory effect was given to the human macrophages when the HepG2 cells (dark control) were applied instead (Figure 5). Our finding is consisting to the discovery by Korbelik and Krosl's [41] work, where the PDT-treated cancer cells could enhance macrophage cytotoxicity.

Conclusions

Taken together, our findings provide the first evidence that Pa-PDT would activate the HLA class I–restricted antigen presentation machinery in HepG2 cells and result in an enhancement of anticancer immunity in the tumor host that would enhance the efficiency of anticancer treatment with Pa-PDT.

References

[1] Harrod-Kim P (2006). Tumor ablation with photodynamic therapy: introduction to mechanism and clinical applications. *J Vasc Interv Radiol* **17**, 1441–1448.
[2] Ackroyd R, Kelty C, Brown N, and Reed M (2001). The history of photodetection and photodynamic therapy. *Photochem Photobiol* **74**, 656–669.
[3] Daniell MD and Hill JS (1991). A history of photodynamic therapy. *Aust N Z J Surg* **61**, 340–348.
[4] Zhu TC and Finlay JC (2008). The role of photodynamic therapy (PDT) physics. *Med Phys* **35**, 3127–3136.
[5] Vogelstein B and Kinzler KW (2004). Cancer genes and the pathways they control. *Nat Med* **10**, 789–799.
[6] Kabingu E, Vaughan L, Owczarczak B, Ramsey KD, and Gollnick SO (2007). $CD8^+$ T cell–mediated control of distant tumours following local photodynamic therapy is independent of $CD4^+$ T cells and dependent on natural killer cells. *Br J Cancer* **96**, 1839–1848.
[7] Kousis PC, Henderson BW, Maier PG, and Gollnick SO (2007). Photodynamic therapy enhancement of antitumor immunity is regulated by neutrophils. *Cancer Res* **67**, 10501–10510.
[8] Krosl G, Korbelik M, and Dougherty GJ (1995). Induction of immune cell infiltration into murine SCCVII tumour by photofrin-based photodynamic therapy. *Br J Cancer* **71**, 549–555.
[9] Takamiya KI, Tsuchiya T, and Ohta H (2000). Degradation pathway(s) of chlorophyll: what has gene cloning revealed? *Trends Plant Sci* **5**, 426–431.
[10] Chan JY, Tang PM, Hon PM, Au SW, Tsui SK, Waye MM, Kong SK, Mak TC, and Fung KP (2006). Pheophorbide a, a major antitumor component purified

from *Scutellaria barbata*, induces apoptosis in human hepatocellular carcinoma cells. *Planta Med* **72**, 28–33.

[11] Oonsivilai R, Cheng C, Bomser J, Ferruzzi MG, and Ningsanond S (2007). Phytochemical profiling and phase II enzyme-inducing properties of *Thunbergia laurifolia* Lindl. (RC) extracts. *J Ethnopharmacol* **114**, 300–306.

[12] Chee CF, Lee HB, Ong HC, and Ho AS (2005). Photocytotoxic pheophorbide–related compounds from *Aglaonema simplex*. *Chem Biodivers* **2**, 1648–1655.

[13] Lee WY, Lim DS, Ko SH, Park YJ, Ryu KS, Ahn MY, Kim YR, Lee DW, and Cho CW (2004). Photoactivation of pheophorbide a induces a mitochondrial-mediated apoptosis in Jurkat leukaemia cells. *J Photochem Photobiol B* **75**, 119–126.

[14] Hajri A, Wack S, Meyer C, Smith MK, Leberquier C, Kedinger M, and Aprahamian M (2002). *In vitro* and *in vivo* efficacy of photofrin and pheophorbide a, a bacteriochlorin, in photodynamic therapy of colonic cancer cells. *Photochem Photobiol* **75**, 140–148.

[15] Jin ZH, Miyoshi N, Ishiguro K, Umemura S, Kawabata K, Yumita N, Sakata I, Takaoka K, Udagawa T, Nakajima S, et al. (2000). Combination effect of photodynamic and sonodynamic therapy on experimental skin squamous cell carcinoma in C3H/HeN mice. *J Dermatol* **27**, 294–306.

[16] Hajri A, Coffy S, Vallat F, Evrard S, Marescaux J, and Aprahamian M (1999). Human pancreatic carcinoma cells are sensitive to photodynamic therapy *in vitro* and *in vivo*. *Br J Surg* **86**, 899–906.

[17] Tang PM, Liu XZ, Zhang DM, Fong WP, and Fung KP (2009). Pheophorbide a based photodynamic therapy induces apoptosis via mitochondrial-mediated pathway in human uterine carcinosarcoma. *Cancer Biol Ther* **8**, 49–55.

[18] Tang PM, Chan JY, Au SW, Kong SK, Tsui SK, Waye MM, Mak TC, Fong WP, and Fung KP (2006). Pheophorbide a, an active compound isolated from *Scutellaria barbata*, possesses photodynamic activities by inducing apoptosis in human hepatocellular carcinoma. *Cancer Biol Ther* **5**, 1111–1116.

[19] Tang PM, Zhang DM, Xuan NH, Tsui SK, Waye MM, Kong SK, Fong WP, and Fung KP (2009). Photodynamic therapy inhibits P-glycoprotein mediated multidrug resistance via JNK activation in human hepatocellular carcinoma using the photosensitizer pheophorbide a. *Mol Cancer* **8**, 56.

[20] Yamashita Y, Moriyasu F, Ono S, Kimura T, Kajimura K, Someda H, Hamato N, Nabeshima M, Sakai M, and Okuma M (1991). Photodynamic therapy using pheophorbide-a and Q-switched Nd:YAG laser on implanted human hepatocellular carcinoma. *Gastroenterol Jpn* **26**, 623–627.

[21] Qiang YG, Yow CM, and Huang Z (2008). Combination of photodynamic therapy and immunomodulation: current status and future trends. *Med Res Rev* **28**, 632–644.

[22] Zhang DM, Wang Y, Tang MK, Chan YW, Lam HM, Ye WC, and Fung KP (2007). Saxifragifolin B from *Androsace umbellata* induced apoptosis on human hepatoma cells. *Biochem Biophys Res Commun* **362**, 759–765.

[23] Tang PM, Chan JY, Zhang DM, Au SW, Fong WP, Kong SK, Tsui SK, Waye MM, Mak TC, and Fung KP (2007). Pheophorbide a, an active component in *Scutellaria barbata*, reverses P-glycoprotein–mediated multidrug resistance on a human hepatoma cell line R-HepG2. *Cancer Biol Ther* **6**, 504–509.

[24] Cho SY, Park PJ, Shin ES, Lee JH, Chang HK, and Lee TR (2009). Proteomic analysis of mitochondrial proteins of basal and lipolytically (isoproterenol and TNF-alpha)–stimulated adipocytes. *J Cell Biochem* **106**, 257–266.

[25] Lee SK, Wong CK, Poon PM, Ip PS, Che CT, Fung KP, Leung PC, and Lam CW (2006). *In vitro* immunomodulatory activities of a newly concocted traditional Chinese medicine formula: VI-28. *Phytother Res* **20**, 883–888.

[26] Campoli M and Ferrone S (2008). HLA antigen changes in malignant cells: epigenetic mechanisms and biologic significance. *Oncogene* **27**, 5869–5885.

[27] Fabris C, Valduga G, Miotto G, Borsetto L, Jori G, Garbisa S, and Reddi E (2001). Photosensitization with zinc (II) phthalocyanine as a switch in the decision between apoptosis and necrosis. *Cancer Res* **61**, 7495–7500.

[28] Hsu CY, Chen YH, Chao PY, Chen CM, Hsieh LL, and Hu SP (2008). Naturally occurring chlorophyll derivatives inhibit aflatoxin B1-DNA adduct formation in hepatoma cells. *Mutat Res* **657**, 98–104.

[29] Evrard S, Keller P, Hajri A, Balboni G, Mendoza-Burgos L, Damge C, Marescaux J, and Aprahamina M (1994). Experimental pancreatic cancer in the rat treated by photodynamic therapy. *Br J Surg* **81**, 1185–1189.

[30] Castano AP, Mroz P, and Hamblin MR (2006). Photodynamic therapy and anti-tumour immunity. *Nat Rev Cancer* **6**, 535–545.

[31] Korbelik M (1996). Induction of tumor immunity by photodynamic therapy. *J Clin Laser Med Surg* **14**, 329–334.

[32] van Duijnhoven FH, Aalbers RI, Rovers JP, Terpstra OT, and Kuppen PJ (2003). The immunological consequences of photodynamic treatment of cancer, a literature review. *Immunobiology* **207**, 105–113.

[33] Canti G, De Simone A, and Korbelik M (2002). Photodynamic therapy and the immune system in experimental oncology. *Photochem Photobiol Sci* **1**, 79–80.

[34] Ren W, Strube R, Zhang X, Chen SY, and Huang XF (2004). Potent tumor-specific immunity induced by an *in vivo* heat shock protein-suicide gene-based tumor vaccine. *Cancer Res* **64**, 6645–6651.

[35] Korbelik M, Sun J, and Cecic I (2005). Photodynamic therapy–induced cell surface expression and release of heat shock proteins: relevance for tumor response. *Cancer Res* **65**, 1018–1026.

[36] Dick TP (2004). Assembly of MHC class I peptide complexes from the perspective of disulfide bond formation. *Cell Mol Life Sci* **61**, 547–556.

[37] Cresswell P, Arunachalam B, Bangia N, Dick T, Diedrich G, Hughes E, and Maric M (1999). Thiol oxidation and reduction in MHC-restricted antigen processing and presentation. *Immunol Res* **19**, 191–200.

[38] Castellino F, Boucher PE, Eichelberg K, Mayhew M, Rothman JE, Houghton AN, and Germain RN (2000). Receptor-mediated uptake of antigen/heat shock protein complexes results in major histocompatibility complex class I antigen presentation via two distinct processing pathways. *J Exp Med* **191**, 1957–1964.

[39] Bendz H, Ruhland SC, Pandya MJ, Hainzl O, Riegelsberger S, Braüchle C, Mayer MP, Buchner J, Issels RD, and Noessner E (2007). Human heat shock protein 70 enhances tumor antigen presentation through complex formation and intracellular antigen delivery without innate immune signaling. *J Biol Chem* **282**, 31688–31702.

[40] Korbelik M, Stott B, and Sun J (2007). Photodynamic therapy–generated vaccines: relevance of tumour cell death expression. *Br J Cancer* **97**, 1381–1387.

[41] Korbelik M and Krosl G (1994). Enhanced macrophage cytotoxicity against tumor cells treated with photodynamic therapy. *Photochem Photobiol* **60**, 497–502.